J|A|C|S
ARTICLES
Published on Web 01/19/2005

Controlled Polymerization in Mesoporous Silica toward the Design of Organic−Inorganic Composite Nanoporous Materials

Minkee Choi, Freddy Kleitz, Dinan Liu, Hee Yoon Lee, Wha-Seung Ahn,‡ and Ryong Ryoo*

Contribution from the Center for Functional Nanomaterials, Department of Chemistry, Korea Advanced Institute of Science and Technology, Daejeon, 305-701, Republic of Korea

Received August 24, 2004; E-mail: rryoo@kaist.ac.kr

Abstract: Free-radical polymerization inside mesoporous silica has been investigated in order to open a route to functional polymer−silica composite materials with well-defined mesoporosity. Various vinyl monomers, such as styrene, chloromethyl styrene, 2-hydroxyethyl methacrylate, and methacrylic acid, were polymerized after impregnation into mesoporous silicas with various structures, which were synthesized using polyalkylene oxide-type block copolymers. The location of the polymers was systematically controlled with detailed structures of the silica framework and the polymerization conditions. Particularly noteworthy is the polymer−silica composite structure obtained by in situ polymerization after the selective adsorption of monomers as a uniform film on silica walls. The analysis of XRD data and the N_2 adsorption isotherms indicates the formation of uniform polymer nanocoating. The resultant polymer−silica composite materials can easily be post-functionalized to incorporate diverse functional groups in high density, due to the open porous structure allowing facile access for the chemical reagent. The fundamental characteristics of the composite materials are substantiated by testing the biomolecule's adsorption capacity and catalytic reactivity. Depending on the structure and composition of polymers, the resultant polymer−silica composite materials exhibit notably distinct adsorption properties toward biomolecules, such as proteins. Furthermore, it is demonstrated that the nanocoatings of polymers deposited on the mesopore walls have remarkably enhanced catalytic activity and selectivity, as compared to that of bulk polymer resins. We believe that, due to facile functionalization and attractive textural properties, the mesoporous polymer−silica composite materials are very useful for applications, such as adsorption, separation, host−guest complexes, and catalysis.

1. Introduction

The enlarged pore size (2−15 nm) of ordered mesoporous silicas compared with microporous zeolites provides us with many opportunities to incorporate diverse organic guest species within highly porous structures in a very systematic and designed manner.[1−11] Organic moieties can readily be functionalized to create active sites in the solid state for catalysis, ion exchange, or adsorption, while taking advantage of the unique textural properties of the mesoporous materials. Such porous composite materials should bring us new scientific possibilities for the study of unique physical and chemical behaviors of molecules confined inside nanospace, which will be significant for the design of innovative materials for chromatography, sensing, electronic and optoelectric devices, or recyclable stable heterogeneous catalysts.

Until now, mesoporous organic−silica composite materials were mostly prepared either by co-condensation reactions of organosilanes directly during the synthesis of the mesoporous material[1−5] or by grafting organosilanes onto pre-prepared mesoporous silica surfaces.[1,6,7] Significant merits of both methods are on the chemical and thermal stability of the organic moieties arising from the strong covalent bonding between the organics and the silica walls. Furthermore, the silica mesopores are usually not blocked after incorporation of the organic species due to a relatively uniform distribution of organic guests. In parallel, several studies were reported on the encapsulation of organic polymers within the channels of mesoporous silica materials.[7−12] For example, Bein and co-worker reported the polymerization of polyaniline inside the mesopore system of

‡ On sabbatical leave from Inha University, Incheon, Korea.

(1) Wight, A. P.; Davis, M. E. *Chem. Rev.* **2002**, *102*, 3589 and references therein.
(2) Inagaki, S.; Guan, S.; Fukushima, Y.; Ohsuna, T.; Terasaki, O. *J. Am. Chem. Soc.* **1999**, *121*, 9611.
(3) Melde, B. J.; Holland, B. T.; Blanford, C. F.; Stein, A. *Chem. Mater.* **1999**, *11*, 3302.
(4) Asefa, T.; MacLachlan, M. J.; Coombs, N.; Ozin, G. A. *Nature* **1999**, *402*, 867.
(5) MacLachlan, M. J.; Asefa, T.; Ozin, G. A. *Chem.—Eur. J.* **2000**, *6*, 2507.
(6) Clark, J. H.; Macquarrie, D. J. *Chem. Commun.* **1998**, 853.
(7) Moller, K.; Bein, T. *Chem. Mater.* **1998**, *10*, 2950.
(8) Wu, C.-G.; Bein, T. *Science* **1994**, *264*, 175.
(9) Moller, K.; Bein, T.; Fischer, R. X. *Chem. Mater.* **1998**, *10*, 1841.
(10) Nguyen, T. Q.; Wu, J. J.; Doan, V.; Schwartz, B. J.; Tolbert, S. H. *Science* **2000**, *288*, 652.
(11) Molenkamp, W. C.; Watanabe, M.; Miyata, H.; Tolbert, S. H. *J. Am. Chem. Soc.* **2004**, *126*, 4476.
(12) Acosta, E. J.; Carr, C. S.; Simanek, E. E.; Shantz, D. F. *Adv. Mater.* **2004**, *16*, 985.

10.1021/ja044907z CCC: $30.25

Scheme 1. Synthesis Strategy for Uniform Polymer Coating on SBA-15 Mesopore Walls[a]

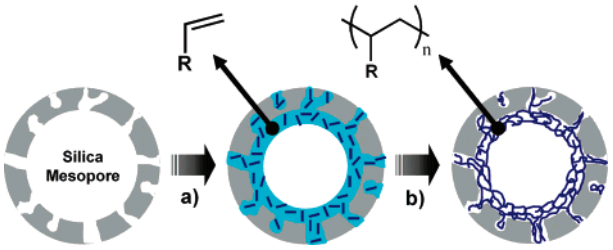

[a] (a) Selective adsorption of vinyl monomers on the silica mesopore walls and (b) subsequent thermal polymerization.

MCM-41.[8] Such a system with conjugated polymers with mobile charge carriers within nanometer-size galleries can be considered as a significant step toward the design of nanoscale electronic devices. Later, Moller et al. investigated the polymerization of methyl methacrylate inside microporous and mesoporous silicas, with the resulting polymer possessing distinct physical properties compared with the bulk polymer.[9] Tolbert and co-workers demonstrated that semiconducting polymers aligned inside mesopores exhibited unique energy transfer and photophysical properties, promising for the preparation of electronic and optoelectric devices.[10,11] In all of these studies, the polymers filled the entire volume of the silica mesopores, resulting, for most of the cases, in nonporous materials. Nevertheless, some remarkable aspects of the nanoscale chemistry and physics of polymers confined within mesoporous channels were revealed. Very recently, Shantz and co-workers reported the synthesis of dendrimers inside the mesoporous silica.[12]

Herein, we suggest an alternative synthesis route toward organic−silica composite materials through radical polymerization of vinyl monomers inside mesoporous silica. In particular, we suggest a systematic and simple methodology to prepare functional materials maintaining the well-defined mesoporosity, locating the polymer entities selectively onto the silica mesopore walls. As shown in Scheme 1, the present scheme uses the incorporation of vinyl monomers, cross-linkers, and radical initiators onto the pore walls of mesoporous silica via wet-impregnation method, followed by equilibration under reduced pressure in order to achieve uniform distribution. The monomers adsorbed on the mesopore walls are subsequently polymerized with heating to form a uniform polymer nanocoating on the surface of the silica framework, using a similar synthesis strategy to the one we described elsewhere with mesoporous carbons[13] as supports. The resultant polymer−silica composite materials are then washed with chloroform and ethanol in order to remove remaining monomers and any detachable polymers.

The present study demonstrates that the location and the structure of the polymers within silica mesopores can be controlled through the modification of the silica structure and polymerization conditions. The synthesis strategy can be applied to the wide range of commercial vinyl monomers, such as styrene, chloromethyl styrene (CMS), 2-hydroxyethyl methacrylate (HEMA), or methacrylic acid (MAA), in the presence of cross-linking agents, such as divinylbenzene (DVB) and ethylene glycol dimethacrylate (EDMA). Moreover, some of the fundamental characteristics of the composite materials are investigated by measuring the biomolecule adsorption capacity and catalytic reactivity. Depending on the structure and composition of polymers, the resultant polymer−silica composite materials exhibit notably distinct adsorption properties toward biomolecules, such as proteins, which is distinct from pure silica material. Furthermore, it is demonstrated that nanocoatings of polymers synthesized on the surface of the mesopores exhibit remarkably enhanced catalytic activity and selectivity, as compared to that of bulk polymer resins.

2. Results and Discussion

I. Control of Polymerization into "Uniform Coating" on Silica Mesopore Walls. As a silica framework for the construction of the composite structure with polymers, SBA-15-type mesoporous silica was prepared through the nonionic assembly pathway under acidic conditions.[14,15] The choice of the SBA-15-type silica is based on the following reason. Recent studies have clearly demonstrated that the large uniform ordered main channels of SBA-15 are actually accompanied by disordered micropore/small mesopores (referred to as "complementary pores") in the pore walls, providing various degrees of interconnectivity between adjacent large pore channels.[15−22] Methods to tailor such complementary pores have been reported in detail.[15,21,22] It is reasonable that such complementary pores would play a crucial role in the stabilization of the polymer layer deposited onto the siliceous mesopore walls. The polymer chains, interpenetrating with the silica framework through the complementary pores, would form a physically inseparable robust polymer network integrated with the silica framework, increasing significantly the stability of the entire polymeric system.

To study the effect of the complementary pores on the polymer deposition, two types of SBA-15 materials were prepared, one sample with large complementary pores and the other with small complementary pores, by employing two different SiO_2:P123 ($EO_{20}PO_{70}EO_{20}$, Aldrich) molar ratios (r) of 45 and 75,[15] respectively. Our preliminary study on SBA-15 silica confirmed that SBA-15 with $r = 45$ contains large (2−4 nm in diameter) complementary pores giving high interconnectivity between adjacent mesopores, whereas SBA-15 with $r = 75$ contains much smaller (<2 nm) complementary pores.[15] Poly(chloromethylstyrene) (PCMS), commonly known as Merrifield resin, was synthesized in the two SBA-15 samples by copolymerization of CMS (80 mol %) and DVB (20 mol %). The monomer loading amounted to 30 wt % of the silica weight. Quantitative determination of organic content by thermogravimetric analysis (TGA) shows that more than 95% of the monomers were converted to stable polymers (Supporting Information S1). Transmission electron microscopy (TEM) investigation reveals that most of the monomers were polym-

(13) Choi, M.; Ryoo, R. *Nat. Mater.* **2003**, *2*, 473.
(14) Zhao, D.; Feng, J.; Huo, Q.; Melosh, N.; Fredrickson, G. H.; Chmelka, B. F.; Stucky, G. D. *Science* **1998**, *279*, 548.
(15) Choi, M.; Heo, W.; Kleitz, F.; Ryoo, R. *Chem. Commun.* **2003**, 1340.
(16) Goltner, C. G.; Smarsly, B.; Berton, B.; Antonietti, M. *Chem. Mater.* **2001**, *13*, 1617.
(17) Ryoo, R.; Ko, C. H.; Kruk, M.; Antochshuk, V.; Jaroniec, M. *J. Phys. Chem. B* **2000**, *104*, 11465.
(18) Jun, S.; Joo, S. H.; Ryoo, R.; Kruk, M.; Jaroniec, M.; Liu, Z.; Ohsuna, T.; Terasaki, O. *J. Am. Chem. Soc.* **2000**, *122*, 10712.
(19) Smarsly, B.; Goltner, C. G.; Antonietti, M.; Ruland, W.; Hoinkis, E. *J. Phys. Chem. B* **2001**, *105*, 831.
(20) Liu, Z.; Terasaki, O.; Ohsuna, T.; Hiraga, K.; Shin, H. J.; Ryoo, R. *Chem. Phys. Chem.* **2001**, 229.
(21) Shin, H. J.; Ryoo, R.; Kruk, M.; Jaroniec, M. *Chem. Commun.* **2001**, 349.
(22) Galarneau, A.; Cambon, H.; DiRenzo, F.; Ryoo, R.; Choi, M.; Fajula, F. *New J. Chem.* **2003**, *27*, 73.

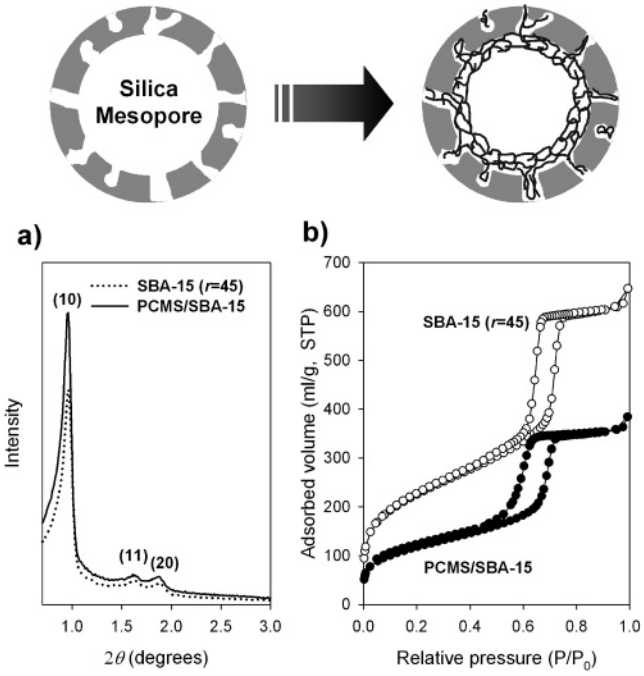

Figure 1. (a) Powder X-ray diffraction patterns and (b) N_2 adsorption isotherms for SBA-15 ($r = 45$) containing large complementary pores, before and after the deposition of cross-linked PCMS inside the silica mesopores.

erized inside the silica mesopores without bulk polymer formation on the external surface of the silica particle (Supporting Information S4).

Pronounced differences in location and homogeneity are observed when the polymers are synthesized within the two different SBA-15 mesoporous systems, as evidenced by powder X-ray diffraction (XRD) and N_2 physisorption analysis. Figure 1 shows the XRD patterns and N_2 adsorption isotherms for SBA-15 with large complementary pores ($r = 45$), before and after deposition of the polymer. As seen in the XRD pattern, the polymer formation in the mesoporous material provokes a significant increase in the intensity of the (10) reflection observed for the two-dimensional (2D) hexagonal mesophase, while the reflections observed at higher angles show no pronounced evolution. The strong increase in diffraction intensity probably originates from an increased X-ray scattering contrast between the walls and the pores of the material.[19,23,24] This observation can be interpreted with polymers filling the complementary porosity present in the walls of SBA-15. Moreover, the marked increase in the intensity ratio between the (10) reflection and higher-indexed reflections points toward thicker mesopore walls,[25] due to uniform coating of polymers on the silica walls. In addition, Barrett−Joyner−Halenda (BJH) analysis[26] of N_2 adsorption−desorption isotherms reveals that the wall thickness increased systematically from 2.9 to 3.7 nm after the polymer deposition, while the mesopore diameter decreased from 7.7 to 6.9 nm. The detailed structural parameters of the materials are given in Table 1.

Table 1. Structural Properties of the SBA-15 and PCMS−SBA-15 Composite Materials

samples[a]	a_0[b] (nm)	D[c] (nm)	h[c] (nm)	V_t[c] (ml/g)	V_{mi}[d] (ml/g)	V_p[d] (ml/g)	S^{BET}[e] (m^2/g)
SBA-15 (45)	10.6	7.7	2.9	0.94	0.10	0.77	770
PCMS−C (45)	10.6	6.9	3.7	0.55	0.04	0.47	404
PCMS−R (45)	10.5	6.7	3.8	0.59	0.09	0.44	583
SBA-15 (75)	10.4	6.9	3.5	0.63	0.09	0.51	518
PCMS−C (75)	10.5	6.2	4.3	0.34	0.03	0.29	195

[a] In the sample notation, C (uniform coating) denotes the composite material synthesized following Scheme 1, while R (random incorporation) denotes the material synthesized following Scheme 2. The number in parentheses indicates the SiO_2/P123 ratio (r) employed for the synthesis of the silica support. [b] The a_0 is the XRD unit cell parameter. [c] D and h are the pore diameter and the pore wall thickness, respectively, determined by the BJH method from the adsorption branch.[25] V_t is the total pore volume calculated by the BJH method. [d] V_{mi} is the micropore volume, and V_p is the primary mesopore volume evaluated using the t-plot method (t-plots are given in Supporting Information, Figure S3). V_p includes a certain contribution from the volume of the complementary pores, so the actual primary mesopore volume is smaller. It should be noted that in the case of polymer composite materials, the calculation might not be accurate. Polymer−silica composite materials can have different surface nature from pure silica material, which was used as a reference system. [e] S^{BET} is the BET surface area.

Here, it is noteworthy that a narrow H1-type adsorption−desorption hysteresis loop typical for SBA-15 is maintained after the polymer loading. Such an H1-type hysteresis loop exhibiting sharp change around $P/P_0 = 0.6-0.7$ is characteristic of uniform mesopores with open cylindrical geometry,[27] which therefore indicates that the polymers were deposited as a uniform coating on the mesopore walls without mesopore blockage. If polymer coatings were formed heterogeneously in thickness along the cylindrical mesoporous channels of the silica sample, the channels would be plugged more or less depending on locations with different thickness. The polymer−silica composite material should then exhibit a broad hysteresis loop in the N_2 adsorption isotherm, compared with SBA-15 silica. However, our result indicates a very narrow hysteresis loop, which is similar to that of silica, except for the P/P_0 position change to low pressure. The position change is due to decreasing pore diameters with polymer coatings.

In contrast, similar experiments with SBA-15 possessing small complementary pores ($r = 75$) reveal that the polymer incorporation results in a much more heterogeneous distribution of the corresponding mesopore diameters (Figure 2). In addition, all of the XRD reflection intensities decreased markedly after polymer incorporation. This change is related to the general tendency of decreasing diffraction intensity when guest species are randomly incorporated inside the mesopores or added at the external surface, inducing a lower scattering contrast.[23,28] Moreover, the distribution of pore diameters results in the pronounced widening of the hysteresis loop (H2-type hysteresis) after polymer deposition, which gives evidence that the mesopores are plugged by polymers.[29,30] Similar observations were made also for various compositions of monomers, such as styrene, HEMA, and MAA. These results indicate that the complementary pores, which are large enough for polymer

(23) Hammond, W.; Prouzet, E.; Mahanti, S. D.; Pinnavaia, T. J. *Microporous Mesoporous Mater.* **1999**, *27*, 19.
(24) Kleitz, F.; Schmidt, W.; Schuth, F. *Microporous Mesoporous Mater.* **2003**, *65*, 1.
(25) Sauer, J.; Marlow, F.; Schuth, F. *Phys. Chem. Chem. Phys.* **2001**, *3*, 5579.
(26) Barrett, E. P.; Joyner, L. G.; Halenda, P. P. *J. Am. Chem. Soc.* **1951**, *73*, 373.
(27) Kruk, M.; Jaroniec, M. *Chem. Mater.* **2001**, *13*, 3169.
(28) Marler, B.; Oberhagemann, U.; Vortmann, S.; Gies, H. *Microporous Mater.* **1996**, *6*, 375.
(29) Van Der Voort, P.; Ravikovitch, P. I.; De Jong, K. P.; Benjelloun, M.; Van Bavel, E.; Janssen, A. H.; Neimark, A. V.; Weckhuysen, B. M.; Vansant, E. F. *J. Phys. Chem. B* **2002**, *106*, 5873.
(30) Kruk, M.; Jaroniec, M.; Joo, S. H.; Ryoo, R. *J. Phys. Chem. B* **2003**, *107*, 2205.

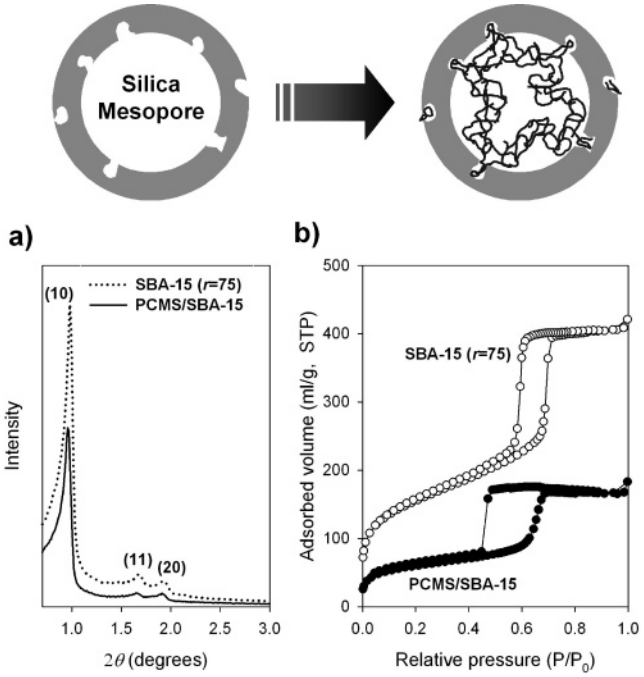

Figure 2. (a) X-ray powder diffraction patterns and (b) N_2 adsorption isotherms for SBA-15 ($r = 75$) containing large complementary pores, before and after the deposition of cross-linked PCMS inside the silica mesopores.

Scheme 2. Synthesis Strategy for Random Incorporation of the Polymer Inside SBA-15 Mesopores[a]

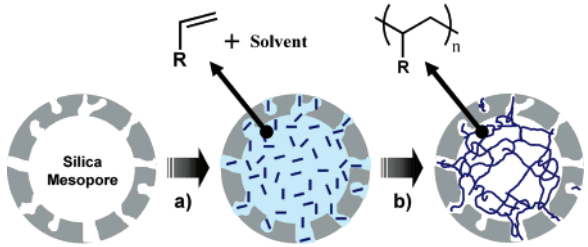

(a) Mesopore filling with the monomers and organic solvent mixture, and (b) thermal polymerization.

incorporation, are important for the stable fixation of polymers onto the silica pore walls.

II. "Random Incorporation" of Polymers inside Silica Mesopores. In the previous section, it was shown that uniform polymer layers could be synthesized as fixed on silica pore walls. The selective monomer adsorption on mesopore walls possessing the large complementary pores was essential for the synthesis of materials having uniform mesopores. Differently, in the present section, we try random incorporation of polymers inside the same silica mesopores by distributing the monomers throughout the entire volume of the silica pores. To demonstrate this, the same monomer mixture (30 wt % loading, 80 mol % CMS with 20 mol % DVB) diluted in toluene was infiltrated into the SBA-15 silica ($r = 45$). The amount of toluene was adjusted so that the total amount of the mixture becomes equal to the total pore volume of the silica sample (Scheme 2). The mixture was heated in sealed tubing, so that the monomers were polymerized in the presence of toluene within the silica mesopores.

After removal of toluene, the resultant sample was characterized by XRD and N_2 adsorption analysis. The XRD patterns and N_2 adsorption isotherms, before and after the polymerization, are presented in Figure 3. XRD reflection intensities decreased significantly after the polymerization, which is indicative of nonselective deposition of the polymers in the mesopores. The broadening and tailing of the hysteresis loop in the N_2 adsorption isotherm clearly indicate that the mesopore diameters are more heterogeneous than those in the case of "uniform coating". The broad distribution of mesopore diameters can be interpreted by silica mesopore "plugging"[29,30] due to the random location of polymers in the 1D mesoporous channel. In addition, the micropore analysis using the t-plot method (Supporting Information S3) revealed that the micropore content (V_{mi}) in the mesopore walls did not decrease after such polymer incorporation (Table 1). This result is in contrast with a marked decrease of V_{mi} in the case of the uniform coating, which can be interpreted by polymer filling in micropores present inside the mesopore walls. We believe that during the solution polymerization in toluene, the polymers are mostly formed in the solvent (toluene) phase occupying the mesopores. Since the polymers are heavily cross-linked and of limited mobility, the polymers are maintained inside the silica mesopores, plugging the mesopores even after the toluene is evaporated.

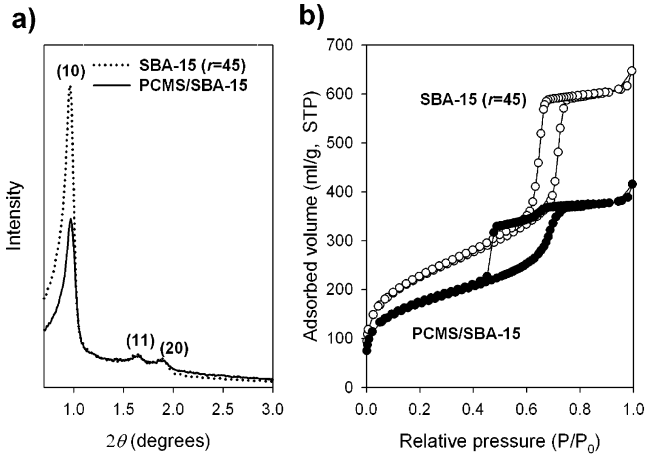

Figure 3. (a) X-ray powder diffraction patterns and (b) N_2 adsorption isotherms for SBA-15 ($r = 45$) containing large complementary pores, before and after random incorporation of PCMS inside the silica mesopores.

III. Post-Functionalization of the Polymer−SBA-15 Silica Composite Material. A rich variety of post-functionalization procedures by organic reactions introducing various functional groups into polymers are currently available to prepare solid catalysts and ion-exchange materials.[31−33] These methods may be applied to the polymer−silica composite materials described herein. For instance, the aforementioned PCMS−SBA-15 can be functionalized through quaternarization with trimethylamine to generate a high density of anion exchange sites. Evidence for the conversion of $-CH_2Cl$ to $-CH_2N^+$ is given by ^{13}C CP-MAS NMR spectra shown in Figure 4. The ^{13}C CP-MAS NMR spectra of the composite materials before and after the quaternarization can be assigned based on literature data.[34] The peaks at 40 ppm are assigned to the backbone methylene and methine carbons, the peak at 47 ppm to the chloromethyl carbon, and the peak at 128 ppm belongs to the protonated aromatic carbons.

(31) Kirschning, A.; Monenschein, H.; Wittenberg, R. *Angew. Chem., Int. Ed.* **2001**, *40*, 650.
(32) McNamara, C. A.; Dixon, M. J.; Bradley, M. *Chem. Rev.* **2002**, *102*, 3275.
(33) Benaglia, M.; Puglisi, A.; Cozzi, F. *Chem. Rev.* **2003**, *103*, 3401.
(34) Law, R. V.; Sherrington, D. C.; Snape, C. E. *Ind. Eng. Chem. Res.* **1995**, *34*, 2740.

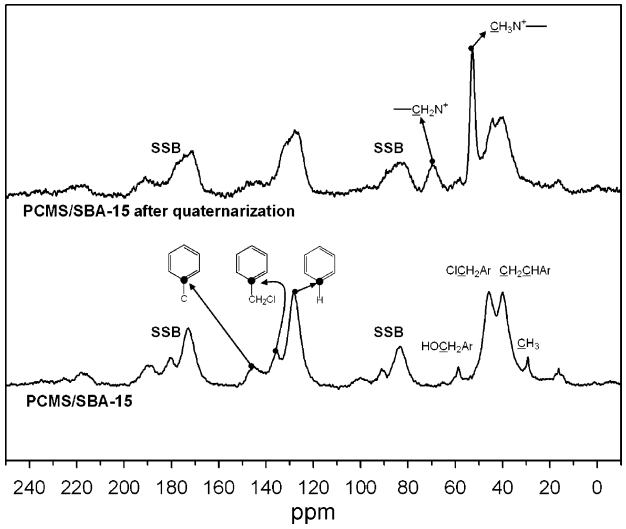

Figure 4. ^{13}C CP-MAS NMR spectra for PCMS−SBA-15 composite material, before and after quaternarization with trimethylamine (SSB: spinning sidebands).

The peak at 136 ppm is assigned to chloromethylated aromatic carbons and the peak at 147 ppm to the quaternary aromatic carbons. After quaternarization, the most prominent feature is the sharp $-N^+CH_3$ resonance at 53 ppm, accompanied by the $-CH_2N^+\equiv$ resonance at 69 ppm and the reduction in intensity of the peak at 47 ppm, which indicates the conversion of the chloromethyl groups into trimethylammonium species.

Quantitative determination of the quaternary ammonium groups was performed with combustion elemental analysis. In the case of the PCMS−SBA-15 with uniform coating (see Section I), the nitrogen content amounted to 3.9 mmol g^{-1} polymer (or 0.9 mmol g^{-1} composite). This value is comparable to the ion-exchange capacity of conventional resins (3−4 mmol g^{-1} polymer). Typically, conventional ion-exchange resins are prepared by quaternarization of Merrifield resins with low cross-linking density (usually less than 5%), in the presence of a swelling agent to allow the access of the trimethylamine inside the polymer matrix.[35−37] The high functionalization capacity of the new composite material, despite 20% cross-linking density and no swelling agent, demonstrates that the accessibility of the trimethylamine to the polymer surface is facile because of the highly porous mesostructure of the material. As a result of thin coating of polymers with uniform mesoporosity, these materials are expected to show greatly improved contact efficiency for guest molecules and therefore faster ion-exchange behavior compared to that of traditional resins.[38]

On the contrary, the PCMS−SBA-15 with random incorporation (see Section II) showed much lower amounts of functionalized groups. Elemental analysis reveals that the nitrogen content amounted to 2.2 mmol g^{-1} polymer (or 0.5 mmol g^{-1} composite). This low functionalization ability indicates that the diffusion of the trimethylamine to the polymer moiety is hindered due to the mesopore blockage.

IV. Adsorption and Catalytic Properties. Mesoporous silicas with other structures possessing complementary porosity are available through the synthesis route using block copolymers, in addition to the 2D hexagonally ordered mesoporous structure of SBA-15. For example, mesoporous silicas with cubic *Ia*3*d*,[39] *Im*3*m*, and *Fm*3*m*[40] structures were recently synthesized with the addition of butanol into polyalkylene oxide-type structure-directing agent solutions. Pore diameters of such silicas can be controlled in a wide range, depending on various synthesis conditions, such as the structure-directing agents, hydrothermal treatments, and cosurfactants. These silicas with complementary pores can lead to the synthesis of highly ordered mesoporous polymer−silica composite materials with various pore structures and controllable pore diameters (see Supporting Information). The tunability of pore structures as well as facile functionalization ability of the polymer−silica composites offers clear advantages for applications in adsorption and catalysis.

Here, fundamental characteristics of the composite materials were substantiated by investigating adsorption capacity for biomolecules and selectivity in catalytic reactions. As a test platform, we investigated the adsorption capacity of the composite materials for bovine hemoglobin and the catalytic activity for the esterification of benzyl alcohol with hexanoic acid. A particularly interesting aspect to investigate is the difference of functions between the polymers confined in the mesopores of the composite materials and those in bulk polymer resins. We demonstrate below that depending on the loading and location of the polymers inside the silica mesopores (i.e., uniform coating and random incorporation), the resulting adsorption and catalytic properties of the composite materials can be modified significantly.

Bovine Hemoglobin Adsorption. In recent years, extensive research has been performed on the encapsulation of guest molecular species inside mesoporous silicas.[7−12,41−45] Especially, mesoporous silicas have attracted large scientific attention as a support for proteins for the fabrication of biosensors and catalysts, due to large pore sizes and easy functionalization.[41−45] Reports have shown that an enzyme could exhibit exceptionally enhanced stability[44,46] and greater catalytic activity[42,44] when encapsulated in mesoporous silica. To control the efficiency of immobilization and the function of proteins, surface modification without mesopore blockage is of prime importance. In the present work, we show that uniform coating of the pore walls with various polymers is an effective means to modify the surface nature of the silica mesopores, as exemplified by the adsorption behavior of the composite materials toward bovine hemoglobin (MW = 64 500, isoelectric point pI = 6.8). The hemoglobin, which is chosen as a model biomolecule, was recently proven to be a promising system for the fabrication of an amperometric biosensing system for the detection of H_2O_2 and NO_2^-.[45]

The uptake of hemoglobin was studied with polymer−SBA-15 composite materials having various compositions, synthesized following the different synthesis strategies described above. The polymer compositions and structural parameters are given in

(35) Dorfner, K. *Ion Exchangers*; Walter de Gruyter: Berlin, 1991.
(36) Wheaton, R. M.; Harrington, D. F. *Ind. Eng. Chem.* **1952**, *44*, 1796.
(37) Pepper, K. W. *J. Appl. Chem.* **1951**, *1*, 124.
(38) Economy, J.; Dominguez, L. *Ind. Eng. Chem. Res.* **2002**, *41*, 6436.
(39) Kleitz, F.; Choi, S. H.; Ryoo, R. *Chem. Commun.* **2003**, 2136.
(40) Kleitz, F.; Solovyov, L. A.; Anilkumar, G. M.; Choi, S. H.; Ryoo, R. *Chem. Commun.* **2004**, 1536.
(41) Han, Y.-J.; Stucky, G. D.; Butler, A. *J. Am. Chem. Soc.* **1999**, *121*, 9897.
(42) Deere, J.; Magner, E.; Wall, J. G.; Hodnett, B. K. *Chem. Commun.* **2001**, 465.
(43) Yiu, H. H. P.; Botting, C. H.; Botting, N. P.; Wright, P. A. *Phys. Chem. Chem. Phys.* **2001**, *3*, 2983.
(44) Lei, C.; Shin, Y.; Liu, J.; Ackerman, E. J. *J. Am. Chem. Soc.* **2002**, *124*, 11242.
(45) Dai, Z.; Liu, S.; Ju, H.; Chen, H. *Biosens. Bioelectron.* **2004**, *19*, 861.
(46) Zhou, H.-X.; Dill, K. A. *Biochemistry* **2001**, *40*, 11289.

Table 2. Polymer Compositions and Structural Properties of Various Polymer−SBA-15 Composite Materials

Samples [a]	Monomer (80 mol%)	Crosslinker (20 mol%)	D [d] (nm)	V_t [d] (ml/g)	S^{BET} [e] (m^2/g)	S^{ext} [f] (m^2/g)
SBA-15	-	-	7.7	0.94	770	44
Tm-PCMS-C [b]	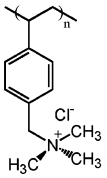	DVB	6.9	0.54	380	32
PS-C	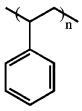	DVB	6.7	0.54	381	31
PHEMA-C	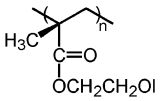	EDMA	6.7	0.53	352	25
PMAA-C	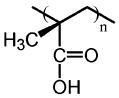	EDMA	6.7	0.51	370	16
Tm-PCMS-R [b]	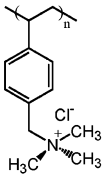	DVB	6.4	0.58	530	43
PHEMA-R	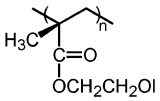	EDMA	5.5	0.50	486	32
PS-F [c]	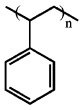	DVB	-	0.02	9	-

[a] The SiO_2/P123 ratio (r) employed for the synthesis of all silica supports was 45. In the synthesis of all composite materials, the polymer loading was fixed to 30 wt % relative to silica weight. In the sample notation, C (uniform coating) denotes the composite material synthesized following Scheme 1, while R (random incorporation) denotes the material synthesized following Scheme 2. [b] Tm−PCMS materials were prepared by reacting PCMS−SBA-15 composite materials (Table 1) with trimethylamine after the polymerization. [c] PS−F sample was prepared by polymerizing 100 wt % monomer relative to silica weight to fill entirely the silica mesopores. [d] D is the pore diameter determined by the BJH method from the adsorption branch.[25] V_t is the total pore volume calculated by the BJH method. [e] S^{BET} is the BET surface area. [f] S^{ext} is the external surface area calculated from t-plot method.

Table 2. The adsorption capacities are plotted as a function of the equilibrium concentration in Figure 5. The results reveal that the protein molecules can be adsorbed in the mesopores of the polymer−silica composite materials with various compositions if the polymers are uniformly coated. In particular, the composite material functionalized with positively charged trimethylammonium groups (Tm−PCMS−C) exhibits the highest adsorption capacity for the protein, while materials with negatively charged functional groups, such as carboxylic acid groups (PMAA−C), show much lower uptakes. Composite materials with neutral polymer moieties (PS−C and PHEMA−C) and purely siliceous mesoporous SBA-15 show intermediate adsorption capacities. These trends may be explained on the basis of the electrostatic interaction between the polymer moiety and hemoglobin molecules. Since pI of the hemoglobin is 6.8, the protein molecules are negatively charged at pH 9.1. Negatively charged hemoglobin interacts more strongly with polymer moieties having positively charged functional groups.

Particularly noteworthy is that the composite material with random polymer incorporation (Tm−PCMS−R, PHEMA−R) exhibits very low adsorption capacity among the samples investigated. The total pore volume of the random incorporation sample is similar to that of the uniform coating sample. However, the former shows a much lower adsorption capacity than the latter. The pronounced adsorption difference between the two samples gives additional evidence that the open

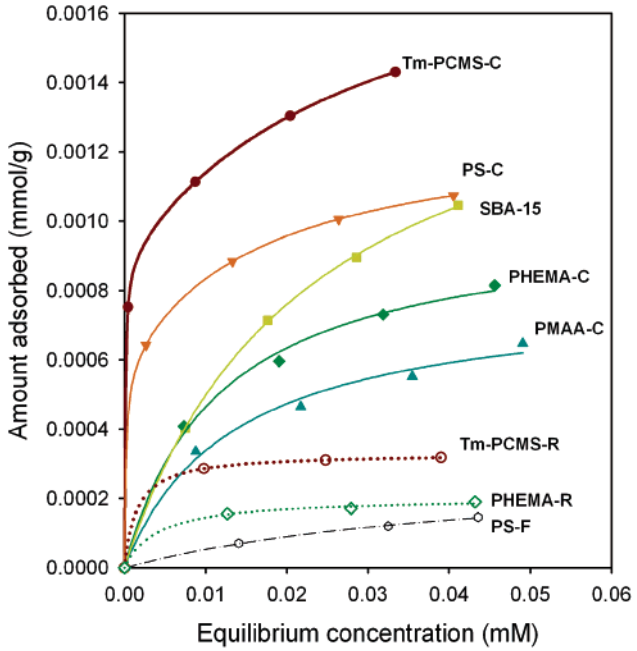

Figure 5. Adsorption isotherms of bovine hemoglobin on SBA-15 (r = 45) and various polymer−SBA-15 composite materials at pH 9.1. The adsorbed hemoglobin quantity was calculated based on the weight of composite material.

mesoporous structure was retained after polymerization in the case of the uniform coating, allowing space for the uptake of large protein molecules inside the porous structure. Conversely, in the case of the random incorporation, the polymers that formed inside the siliceous mesopores blocked the diffusion of the large protein molecules into the porous channels. As expected, the composite material with pores completely filled with polystyrene (PS−F) exhibits the lowest capacity for protein adsorption. The small observed adsorption capacity for the protein is due to protein adsorption on the external surface of the material.

Acid Catalysis with Sulfonated Polystyrene−SBA-15 Composite Materials. The route to polymer−silica composite mesoporous materials can offer a remarkable "flexibility" in the design of solid catalysts. Parameters, such as loading, composition, and location of polymers, as well as structural properties of the silica support, can be controlled to tailor and optimize the catalytic efficiency of the system. In this section, we examine the catalytic properties of sulfonated polystyrene−SBA-15 composite materials for the esterification of benzyl alcohol with hexanoic acid (Scheme 3). The experimental details for the sulfonation reaction of polystyrene−SBA-15 samples are given in the Experimental Section. The structural properties and acid group densities are reported in Table 3. The esterification reaction was chosen since this reaction with a solid catalyst is relevant in both industry and academia.[47−49] Acid-catalyzed esterification produces ether as a byproduct due to a dehydrative condensation reaction between two alcohol molecules, thus permitting us to compare both selectivity and activity of diverse catalysts. Evaluation of the selectivity can be used as a kind of "barometer" to estimate how uniform the microenvironments surrounding catalytic active sites are.[49] It has been acknowledged that chemical and spatial uniformity of reactive sites in heterogeneous catalysts is of utmost importance for obtaining high selectivity and reactivity.[50]

Table 3. Structural Properties and Acid Group Densities for Catalysts Containing Sulfonic Acid Groups

samples[a]	a_0[b] (nm)	D[c] (nm)	h[c] (nm)	V_t[c] (ml/g)	S^{BET}[d] (m^2/g)	acid content[e] (mmol/g composite)
10-SPS−C	10.1	6.7	3.4	0.55	425	0.51
20-SPS−C	10.1	6.5	3.6	0.42	331	0.77
30-SPS−C	9.9	6.1	3.8	0.35	323	1.2
Amberlyst-15						4.5
10-SPS−R	10.0	6.9	3.1	0.72	558	0.19

[a] The SiO_2/P123 ratio (r) employed for the synthesis of all silica supports was 45. In the sample notation for sulfonated polystyrene−SBA-15 composites (SPS), the numbers indicate the initial loading (wt %) of polystyrene relative to silica weight. C (uniform coating) denotes the composite material synthesized following Scheme 1, and R (random incorporation) denotes the material synthesized following Scheme 2. [b] The a_0 is the XRD unit cell parameter. [c] D and h are the pore diameter and the pore wall thickness, respectively, determined by the BJH method from the adsorption branch.[25] V_t is the total pore volume calculated by the BJH method. [d] S^{BET} is the BET surface area. [e] Accessible acid group contents were determined by titration with standardized aqueous NaOH solution.

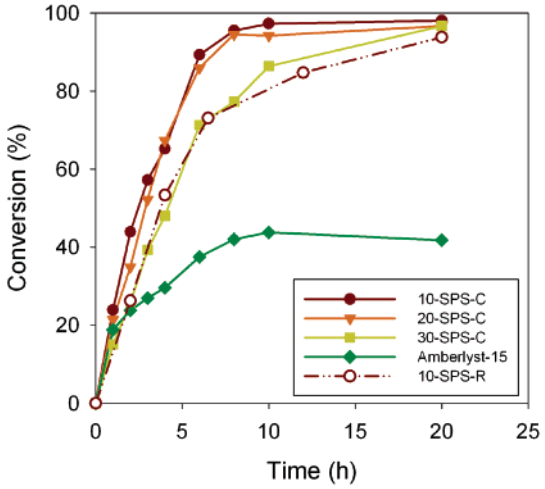

Figure 6. Total product conversion for various catalysts as a function of reaction time.

The esterification of benzyl alcohol with hexanoic acid was performed in toluene at 75 °C, following the procedure reported elsewhere.[49] The acid-catalyzed reaction was monitored using gas chromatography (GC), and all reactions were performed with a catalyst loading of 5 mol % H^+ sites relative to the substrate. Total product yields for the catalysts as a function of reaction time are shown in Figure 6. The results show that nearly quantitative conversion was achieved after 20 h with the sulfonated polystyrene−SBA-15 composites (denoted as SPS), while no more products were obtained after 40% conversion with the Amberlyst-15 resin catalyst. The low conversion with Amberlyst-15 is attributed to the consumption of benzyl alcohol due to strong adsorption and oligomerization in micropores, in the case of bulk polymer resins.[49] The distinct difference in catalytic activity between the mesoporous composite materials and bulk resins is remarkable. The higher activity of the mesoporous material can be rationalized by the open mesoporous structure that provides much more easily accessible catalytic sites than a gel-type bulk polymer resin.

(47) Harmer, M. A.; Sun, Q. *Appl. Catal., A* **2001**, *221*, 45.
(48) Dufaud, V.; Davis, M. E. *J. Am. Chem. Soc.* **2003**, *125*, 9403.
(49) Xu, Y.; Gu, W.; Gin, D. L. *J. Am. Chem. Soc.* **2004**, *126*, 1616.
(50) Thomas, J. M. *Angew. Chem., Int. Ed. Engl.* **1988**, *27*, 1673.

Scheme 3. Acid-Catalyzed Esterification Reaction of Benzyl Alcohol with Hexanoic Acid

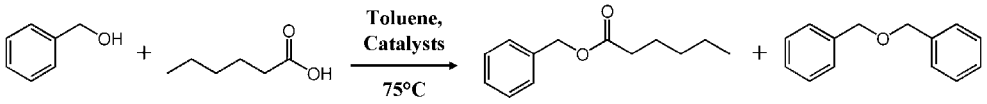

Interesting features appear as the selectivity between the final products is concerned (Figure 7). The polymer−SBA-15 materials with uniform polymer coating (SPS−C) exhibit much higher ester/ether selectivity in the range of 11:1−51:1 (mol/mol) than that with Amberlyst-15 (7:1 mol/mol). Notably, the selectivity of the composite materials increases remarkably, as the polymer loading decreases from 30 to 10 wt %. Such dramatic change in selectivity among the composite samples is difficult to explain simply with their difference in pore diameter because the SPS−C catalyst samples show only a small decrease in mesopore diameters with increasing polymer loading. The selectivity difference indicates that there are certain effects due to a different concentration of the catalytic active sites or the polymer concentration inside the mesoporous channels, which needs more detailed investigation.

The esterification reaction also goes to completion when mesoporous silica is loaded with 10 wt % polymer in the random incorporation way (10-SPC−R). However, the reaction is slower than that of the uniform coating sample (10-SPC−C). Furthermore, the ester selectivity is much lower (13:1 versus 51:1, as shown in Figure 7). The significantly higher selectivity of 10-SPC−C might be rationalized with a more uniform microenvironment of the catalytic sites. In the case of random incorporation, the broad pore-size distribution suggests that micropores and mesopores with different diameters could form between polymer domains of various thicknesses inside the silica mesopores. That is, the local polymer structure would be much more heterogeneous than polymers uniformly coated on the silica framework. Here again, the coated composite polymer−silica materials are proven to be superior to the polymers randomly distributed and agglomerated inside the mesopores.

3. Conclusion

A methodology to control the location of organic polymers within mesoporous silica was developed for the synthesis of functional polymer−silica composite materials with well-defined mesopores. In particular, polymer−silica composite materials possessing uniform mesoporosity can be obtained via in situ free-radical polymerization, after vinyl monomers are adsorbed as a thin layer on the pore walls of mesoporous silicas. Our result indicates that the use of silica with "complementary" pores interconnecting adjacent mesoporous channels is important for the success of this approach because the polymer layer can acquire high stability through the formation of an interpenetrating network between the silica framework and the polymers. Such a polymer layer can subsequently be functionalized through suitable organic reactions to introduce diverse functional groups in high density. For example, the polymer layer modified the adsorption behavior toward biomolecules, such as proteins, for instance. Moreover, the polymer layer exhibited remarkably enhanced catalytic activity and selectivity for esterification of benzyl alcohol using hexanoic acid, compared with bulk polymer resins or polymers randomly filled inside the mesopores of silica.

The synthesis strategy using vinyl monomers can provide us with remarkable advantages of incorporating organic moieties within the mesoporous silicas via the formation of a robust C−C bond rather than hydrolysis-susceptible siloxane bonds. The synthesis strategy using polymer deposition also affords excellent flexibility in the design of functional mesoporous materials. Various commercial vinyl monomers are available, and their copolymerization can be envisaged to prepare multifunctional materials. It would also be possible to deposit different polymers, layer by layer, to form multilayered polymer structures on the surface of silica mesopore walls. We believe that due to facile functionalization and attractive textural properties, the present approach would be useful for the development of high-performance systems for applications, such as adsorption, separation, sensing, host−guest complexes, and catalysis, in addition to the conventional method to functionalize mesoporous silica using organosilanes.

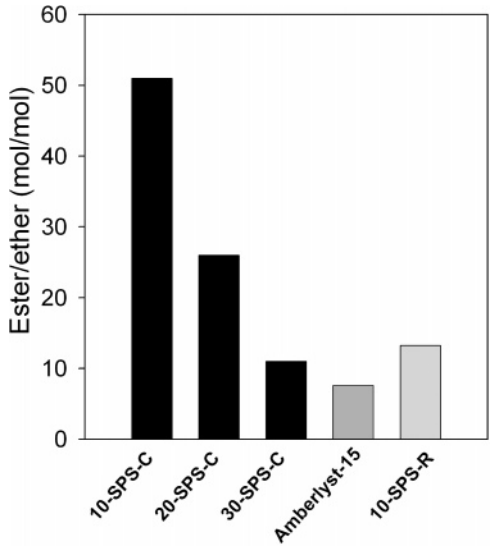

Figure 7. Ester/ether selectivity (mol/mol) of the final products after 20 h reaction.

4. Experimental Section

Synthesis of Mesoporous SBA-15 Materials. All SBA-15 samples were prepared by using $EO_{20}PO_{70}EO_{20}$ (Pluronic P123, Aldrich) as a structure-directing agent and TEOS (ACROS, 98%) as the silica precursor. Two types of SBA-15 materials, with high and low complementary porosity, were prepared by using a different SiO_2:P123 molar ratio (r) of 45 and 75, following the procedure previously reported.[15] High-quality SBA-15 samples were obtained within this range of SiO_2:P123 molar ratio. In a typical synthesis for SBA-15 (r = 45), 3.46 g of P123 was dissolved in 62.8 g of distilled water and 2.0 g of concentrated HCl (35%), to which 5.58 g of TEOS was subsequently added at once under stirring at 35 °C. For the synthesis of SBA-15 (r = 75), 9.3 g of TEOS was added to the same solution under the above conditions. The mixture was stirred at 35 °C for 24 h and subsequently heated for 24 h at 100 °C under static conditions. The solid product was then filtered and dried without washing at 100 °C. To remove the template, the solid was slurried in an ethanol/HCl mixture, filtered, dried, and then calcined in airflow at 550 °C.

Polymerization inside the Mesoporous Silica. Chloromethylstyrene (CMS, Aldrich, 90%) and divinylbenzene (DVB, Aldrich, 98%) were purified on an alumina column to remove the polymerization inhibitors.

Calcined mesoporous silicas were used after overnight vacuum degassing at 300 °C. Typically, monomer mixtures amounting up to 30 wt % of the silica weight were added to 1 g of activated mesoporous silica following the wet-impregnation procedure using dichloromethane as solvent. A typical synthesis follows: 0.228 mL of CMS (80 mol %) was dissolved together with 0.058 mL of DVB (20 mol %) and 0.012 g (3% relative to total vinyl group) of *a*,*a*′-azoisobutyronitrile (AIBN, Aldrich, 98%) in 1.50 mL of dichloromethane. After impregnation of the solution, the powder was dried at 40 °C to selectively remove dichloromethane for 2 h. The sample was then subjected to freeze−vacuum−thaw cycles using dry ice/acetone to remove residual dichloromethane and air. The sample was sealed under vacuum in Pyrex tubing and equilibrated for 6 h at room temperature. The samples were subsequently heated for polymerization. The temperature scheme for the polymerization is 4 h at 60 °C, 1 h at 100 °C, and finally 1 h at 120 °C. The resultant samples were extensively washed with chloroform and ethanol, followed by drying at 80 °C for prolonged time. To study the correlation between monomer distribution inside the mesopores and the resultant polymer structure, the same monomer mixture (30 wt % loading, 80 mol % CMS and 20 mol % DVB) was polymerized inside SBA-15 ($r = 45$) in the presence of 0.7 mL of toluene, which filled the entire volume of the silica mesopores. After impregnation of the solution, the sample was subjected to freeze−vacuum−thaw cycles using liquid nitrogen. After equilibration, the sample was subsequently heated for 6 h at 60 °C for the polymerization. The resultant sample was washed with chloroform and ethanol and dried at 80 °C.

For other compositions of monomers, such as styrene, 2-hydroxyethyl methacrylate (HEMA), or methacrylic acid (MAA), the same synthesis conditions can be applied without any modification.

Quaternarization of PCMS with Trimethylamine. One gram of each PCMS−SBA-15 composite was dispersed in a mixture of 1.5 mL of trimethylamine (Aldrich, 40 wt % aqueous solution) and 50 mL of acetonitrile. The solution was heated under stirring at 80 °C for 6 h in an autoclave. The resulting product was filtered and washed thoroughly with acetonitrile. Nitrogen content in the product was analyzed by combustion elemental analysis after vacuum-drying. Combustion elemental analysis was performed by using EA1110-FISONS Elemental Analyzer equipped with a TCD detector.

Bovine Hemoglobin Adsorption. For the protein adsorption experiment, a standard solution was prepared by dissolving bovine hemoglobin (MW = 64 500, Sigma) in a borate buffer solution (pH 9.1). Twenty milligrams of polymer−silica composite materials was suspended in 1 cm^3 to achieve concentrations between 0 and 4 mg cm^{-3} and shaken for 48 h at 37 °C. After centrifugation, the protein concentration of the supernatant solution was analyzed by using UV−vis absorbance at $\lambda = 410$ nm with a Shimadzu UV-3100S spectrophotometer.

Acid-Catalysis using Mesoporous Sulfonated Polystyrene−SBA-15. Catalysts were prepared by polymerization of styrene (80 mol %) and DVB (20 mol %) with AIBN (3% relative to total vinyl group) inside SBA-15, followed by sulfonation using concentrated H_2SO_4. Three samples were prepared by uniform deposition of cross-linked polystyrene inside SBA-15 ($r = 45$), with total polymer loading of 10, 20, and 30 wt %. In a typical synthesis (30 wt % loading), 1 g of SBA-15 was impregnated with 0.250 mL of styrene (80 mol %) and dissolved with 0.078 mL of DVB (20 mol %) and 0.016 g (3% relative to total vinyl group) of AIBN in 1.50 mL of dichloromethane. After impregnating the solution, the silica sample was dried at 40 °C for 2 h to remove dichloromethane and was heated for polymerization following the same temperature program used for the deposition of PCMS described above.

A sample was also prepared by polymerizing a 10 wt % styrene and DVB mixture in the presence of toluene, which occupied the entire volume of the silica mesopores, to fill the mesopores randomly with polymers. For this synthesis, 1 g of silica was impregnated with 0.084 mL of styrene (80 mol %) and was dissolved with 0.026 mL of DVB (20 mol %) and 0.005 g (3% relative to total vinyl group) of AIBN in 0.8 mL of toluene. After impregnation of the solution, the sample was subjected to freeze−vacuum−thaw cycles using liquid nitrogen. After equilibration for 6 h at 35 °C, the sample was subsequently heated for 6 h at 60 °C for the polymerization. All samples were extensively washed with chloroform and ethanol and dried at 80 °C for a prolonged period.

All polystyrene−SBA-15 samples were sulfonated in concentrated H_2SO_4 at 100 °C for 6 h. After extensive washing with distilled water, samples were vacuum-dried at room temperature overnight. In addition to the above four composite materials, bulk Amberlyst-15 (Aldrich) resin was also used as a catalyst. To determine the density of accessible H^+ site, preweighed catalysts were stirred with saturated NaCl aqueous solution for 24 h at ambient temperature. The supernatant solution was titrated with a standard NaOH solution.

The esterification reactions were carried out in an Schlenk flask with an equimolar ratio of benzyl alcohol and 1-hexanoic acid in dry toluene. The initial concentration of the two reactants were both 0.5 M. The solid acid catalyst loading was 5 mol % relative to the reactants, based on the number of accessible H^+ sites in the resins, as determined by titration. A certain amount of *n*-hexadecane was added to each reaction mixture to serve as the internal standard for quantitative GC analysis. The reactions were initiated by heating with stirring in a 75 °C temperature-regulated oil bath. The progress of the reactions was monitored with gas chromatography (Hewlett-Packard 5890 Series II gas chromatograph equipped with a flame ionization detector and a packed column with 10% SE−30) by regularly taking samples of the supernatant.

Physical Measurements and Instrumentation. XRD patterns were recorded using a Rigaku Multiflex diffractometer equipped with Cu Kα radiation (40 kV, 40 mA). XRD scanning was performed under ambient conditions at steps of 0.01° and an accumulation time of 1 s per step. N_2 adsorption isotherms were measured at 77 K using a Quantachrome AS-1MP volumetric adsorption analyzer. Before the adsorption measurements, all samples were outgassed for 12 h at 353 K in the degas port of the adsorption analyzer. Pore size distributions were analyzed following the BJH algorithm. Thermogravimetric analysis (TGA) was performed using a TGA 2050 thermogravimetric analyzer (TA Instruments). During the measurement, temperature was increased to 1173 K with the rate of 10 K/min. Solid-state CP-MAS ^{13}C NMR measurements were recorded on a solid-state Bruker DSX-400 NMR spectrometer using a Bruker 4 mm CP-MAS probe. A typical spinning rate for CP-MAS experiments is 4.5 kHz. A 2 ms cross polarization contact time was used to acquire ^{13}C CP-MAS spectra with a repetition delay of 3 and 10 000 scans. ^{13}C was referenced to tetramethylsilane.

Acknowledgment. This work was supported in part by the Creative Research Initiative Program of the Korean Ministry of Science and Technology, and by the School of Molecular Science through the Brain Korea 21 project. We also thank KBSI for the measurement of ^{13}C CP-MAS NMR spectrum.

Supporting Information Available: TGA measurements of PCMS−SBA-15 composite; XRD patterns and N_2 adsorption isotherms for PCMS−SBA-15 composites with different polymer content; t-plots for silica and polymer−silica composite materials; TEM images of the composite material (PCMS−C (45)); XRD patterns and N_2 adsorption isotherms for polymer−silica composites with different pore structure and pore diameter (PDF). This material is available free of charge via the Internet at http://pubs.acs.org.

JA044907Z